Presteady State Kinetics of ATP Hydrolysis by *Escherichia coli* Rho Protein Monitors the Initiation Process

Yong-Joo Jeong[†] and Dong-Eun Kim[*]

[†]*Department of Bio and Nanochemistry, Kookmin University, Seoul 136-702, Korea*
Department of Biotechnology and Bioengineering, and Department of Biomaterial Control, Dong-Eui University, Busan 614-714, Korea. [*]*E-mail: kimde@deu.ac.kr*
Received December 5, 2005

Escherichia coli transcription termination factor Rho catalyzes the unwinding of RNA/DNA duplex in reactions that are coupled to ATP binding and hydrolysis. We report here the kinetic mechanism of presteady state ATP binding and hydrolysis by the Rho-RNA complex. Presteady state chemical quenched-flow technique under multiple turnover condition was used to probe the kinetics of ATP binding and hydrolysis by the Rho-RNA complex. The quenched-flow presteady state kinetics of ATP hydrolysis studies show that three ATPs are bound to the Rho-RNA complex with a rate of $4.4 \times 10^5\ M^{-1}s^{-1}$, which are subsequently hydrolyzed at a rate of $88\ s^{-1}$ and released during the initiation process. Global fit of the presteady state ATP hydrolysis kinetic data suggests that a rapid-equilibrium binding of ATP to Rho-RNA complex occurs prior to the first turnover and the chemistry step is not reversible. The initial burst of three ATPs hydrolysis was proposed to be involved in the initialization step that accompanies proper complex formation of Rho-RNA. Based on these results a kinetic model for initiation process for Rho-RNA complex was proposed relating the mechanism of ATP binding and hydrolysis by Rho to the structural transitions of Rho-RNA complex to reach the steady state phase, which is implicated during translocation along the RNA.

Key Words : *E. coli* transcription termination factor Rho, Presteady state kinetics, Global fit, Rapid-equilibrium, Chemical quenched-flow technique

Introduction

Escherichia coli transcription termination factor Rho catalyzes the unwinding of RNA/DNA duplex in reactions that are coupled to ATP binding and hydrolysis.[1,2] Based on quaternary structure of the Rho protein, it belongs to a class of helicases with a homology to the hexameric helicases.[3,4] The Rho protein requires a specific Rho loading site to initiate and bind to the RNA. After initiation, the Rho protein is believed to translocate unidirectionally along the RNA to disrupt the transcriptional complex.[4,5] Rho is therefore a motor protein that couples ATP hydrolysis to movement along RNA, which is similar to DNA and RNA helicases, and Rho can disrupt RNA/DNA duplexes. Although Rho is composed of six identical subunits, the enzyme binds three ATPs in a single class of catalytically competent sites,[6] and an additional class of three ATP-binding sites with a distinct kinetic and thermodynamic property.[7-9] It has been shown that the RNA-dependent ATPase activity is essential for the transcription termination function of Rho and the ATP hydrolysis reaction is stimulated by the RNA homopolymer poly (C) RNA.[8,9]

There has been a great interest in understanding the mechanism of ATP hydrolysis by hexameric helicases. The mechanism of ATP hydrolysis has been studied by pre-steady-state kinetic methods by us and other groups. Based on these studies Stitt has proposed that Rho hexamer binds three ATPs and hydrolyzes the three ATPs in a sequence using a mechanism similar to the binding change mechanism of the F1-ATPase.[6] Our studies previously have shown that Rho protein in addition to the three catalytic sites contain three slowly hydrolyzing sites, coined the noncatalytic sites, based on similar sites in the F1-ATPase.[9] The ATPs bound to the noncatalytic sites are hydrolyzed with a rate of 15-fold slower than the ATPase turnover rate of $30\ s^{-1}$ at 18 °C.[8]

Our studies reported here indicate that the presteady state kinetics is highly dependent on the incubation conditions. Linear kinetics was observed when the reaction was initiated with ATP and RNA, a presteady lag was observed when the reaction was initiated with RNA, and burst kinetics was observed when the reaction was initiated with ATP. Based on these results, in this paper we report a detailed presteady state kinetic analysis of the catalytic sites using the rapid chemical quenched-flow method.

Materials and Methods

Protein, RNA Homopolymer, Nucleotide, and Buffer. The Rho protein was over-expressed in *E. coli* strain HB101 carrying the Rho over-expression plasmid pKS26, and purified according to Finger and Richardson with slight modifications.[10,11] The Rho protein concentration was determined by UV absorption at 280 nm using an extinction coefficient of $0.325\ (mg/mL)^{-1}\ cm^{-1}$.[12] The ATP and RNA homopolymer, poly (C), were purchased from Amersham Biosciences. Poly (C) RNA had a reported $S_{20,w}$ value of 7.1 in 0.015 M NaCl, 0.0015 M sodium citrate buffer, pH 7.0 with an average length of 420 bases. Poly (C) RNA concentration was

determined by UV absorption at 269 nm using an extinction coefficient of 6,200 M^{-1} cm^{-1} for the cytosine base. These RNAs were dissolved in TE buffer (40 mM TrisHCl, pH 7.0, 0.5 mM EDTA) and used without further purification. [α-^{32}P]ATP was purchased from Amersham Biosciences and its purity was assessed by polyethyleneimine (PEI)-cellulose TLC and corrected for in all experiments. ATP was purchased from Sigma and used without further purification. ATPase buffer contains 40 mM TrisHCl (pH 7.7), 100 mM KCl, 10 mM $MgCl_2$, 0.1 mM dithiothreitol, and 10% (v/v) glycerol.

Chemical Quenched-flow Measurements of ATP Hydrolysis. Time-course of ATP hydrolysis by the Rho protein was measured using the rapid chemical quenched-flow instrument, RQF-3 (KinTek Corp. State College, PA, U.S.A.). An 8 μL of solution of Rho protein (7.38 μM hexamer in ATPase buffer) and poly (C) RNA (10 μM) was rapidly mixed with an 8 μL of mixture of ATP (20 μM-2.0 mM) and [α-^{32}P]ATP (0.10 μCi/mL) for varying time. The reactions were quenched with 2.0 M formic acid added from the third syringe in the quenched-flow apparatus. Aliquots (1.0 μL) from each acid-quenched reaction at varying time points were spotted on PEI-cellulose TLC, which was developed in 0.4 M potassium phosphate, pH 3.4. The resolved radioactive ATP and ADP were quantified in a PhosphorImager instrument (Amersham Biosciences). Product formation was equal to the radioactivity corresponding to ADP divided by the total radioactivity. To estimate background ATP hydrolysis or hydrolysis at zero time point, the solution containing Rho protein and poly (C) RNA was not included in the reaction and added later to the quenched reaction. This control experiment was repeated three times and the values were averaged and taken as hydrolysis at zero time point.

The amount of product (ADP) was plotted versus the time of the reaction, and the data fit to an single exponential followed by a linear phase as shown below (Eq. 1) to describe the burst kinetics;

$$P(t) = A \times [1-\exp(-k_1 \times t)] + k_2 \times t \quad (1)$$

, where $P(t)$ is the [α-^{32}P]ADP concentration at time t, A is the burst amplitude, k_1 is the rate constant of burst phase, and k_2 is the rate constant of the linear steady state ADP hydrolysis phase.

The presteady state kinetics of ATP hydrolysis upon adding poly (C) RNA were measured in a rapid chemical quenched-flow instrument equipped with three syringe setup at a constant temperature of 18 °C. In the three syringe experiment mode, two delay times were used (KinTek RQF-3 software). An 8 ml solution of Rho protein (8.8 μM hexamer) in ATPase buffer was rapidly mixed with an 8 μL mixture of ATP (4.11 mM) and [α-^{32}P]ATP (0.10 μCi/mL) for 10 s. After incubation for 10 s (the first delay time), the sample was mixed with 31 μL of poly (C) RNA (3.0 μM) in ATPase buffer was added from the third syringe in the quenched-flow instrument. A total of 47 μL reactions were incubated in the reaction loop for varying time (the second delay time, 15 ms-1.0 s) and quenched with 120 μL of 1.0 M formic acid to stop the reaction. Aliquots (1.0 μL) from each acid-quenched reaction at varying time points were withdrawn and the amount of product was analyzed and quantified as described above, and plotted versus the time of the second delay. To estimate ATP hydrolysis in the first delay time prior to mixing with RNA, acid was added from the third syringe instead of the RNA addition. This control experiment was repeated three times and the values were averaged and taken as a zero time point.

Global Fitting of the Proposed Mechanism to the Presteady State ATP Hydrolysis Kinetic Data. The multiple-turnover kinetics of ATP hydrolysis was fit to the ATP binding/hydrolysis mechanism as described by the Scheme 1;

$$H + A \underset{k_{-1}}{\overset{k_1}{\rightleftharpoons}} HA \xrightarrow{k_2} HD \xrightarrow{k_3} H + D \quad \text{(Scheme 1)}$$

, where H is Rho-RNA complex, HA is the Rho-RNA-ATP complex, HD is the Rho-RNA-ADP complex, and D is ADP. The intrinsic rate constants shown in the mechanism were determined by global fitting of the quenched-flow kinetic data collected at various concentrations of ATP. For global fitting, a set of differential equations shown below, which were written for each ATP concentrations, were solved by the numerical integration method with the global nonlinear least-squares fitting performed using the software "Scientist" (MicroMath Research, SLC, UT, U.S.A.)[13];

$$dH/dt = k_{-1}\cdot HA + k_3\cdot HD - k_1\cdot H\cdot A$$
$$dA/dt = k_{-1}\cdot HA - k_1\cdot H\cdot A$$
$$dHA/dt = k_1\cdot H\cdot A - (k_{-1} + k_2)\cdot HA$$
$$dHD/dt = k_2\cdot HA - k_3\cdot HD$$
$$dD/dt = k_3\cdot HD$$

The sum of HD and D at any given time, which was calculated by solving the above differential equations, was fit to the accumulation kinetics of ATP hydrolysis product at each time point obtained experimentally.

Results

Presteady State ATP Hydrolysis is Limited by the RNA Binding Step. Rho protein can bind ATP and poly(C) RNA independently. The presteady state kinetics of ATP hydrolysis with RNA, therefore, can be conducted in three ways (Fig. 1A). In the mixing sequence (a), ATPase reaction was initiated by mixing Rho protein with poly(C) RNA and [α-^{32}P]ATP. In the mixing sequence (b), Rho protein was preincubated with poly(C) RNA and the ATPase reaction was initiated by mixing the Rho-RNA complex with [α-^{32}P]ATP. In the mixing sequence (c), Rho protein was preincubated with [α-^{32}P]ATP and the ATPase reaction was initiated by mixing the Rho-[α-^{32}P]ATP complex with poly(C) RNA. Previously, we have observed that the Rho-catalyzed ATPase rate in the absence of RNA is 10^5-fold slower than the rate in the presence of the RNA (poly(C)-stimulated k_{cat} = 30 s^{-1} and the unstimulated k_{cat} = 3.0 × 10^{-4} s^{-1} at 18 °C).[8,9]

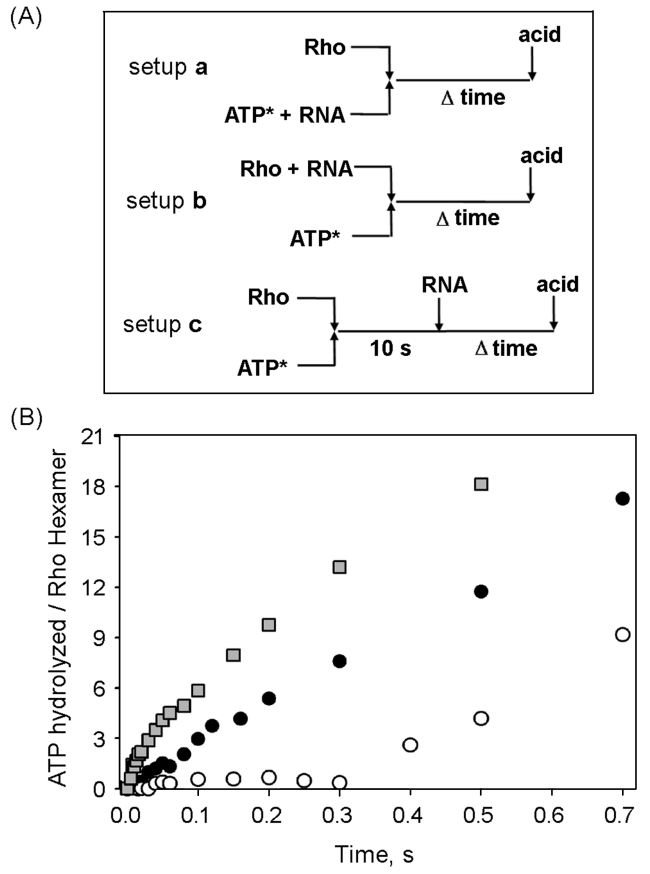

Figure 1. Presteady state acid-quenched kinetics of ATP hydrolysis. (A) The design of each experimental setup is shown. The given concentrations hereafter are the concentrations in the syringe. Setup a; Rho (3.0 μM hexamer) was mixed with [α-^{32}P]ATP (1.4 μM) and poly (C) RNA (4.0 μM) for varying time (Δtime), and the reaction was quenched with 1.0 M formic acid added from the third syringe. Setup b; [α-^{32}P]ATP (2.0 mM) was rapidly mixed with the solution containing Rho (7.4 μM hexamer) and poly (C) RNA (9.9 μM) for varying time, and the reaction was quenched. Setup c; Rho (8.8 μM hexamer) was preincubated with [α-^{32}P]ATP (4.1 mM) for 10 sec. The poly (C) RNA (3.0 μM) was added from the third syringe after 10 s, and the incubation time was varied before the reactions were acid-quenched. (B) The amount of ATP hydrolyzed to ADP per Rho hexamer was plotted as a function of time for each setup of experiment (closed circles; setup a, squares; setup b, and open circles; setup c).

The three types of mixing were carried out in a rapid quenched-flow apparatus, where mixing and quenching (with an acid) can be carried out from 5 msec to several seconds. When the reaction was mixed under condition (a), linear ATP hydrolysis kinetics without any indication of a presteady state burst or lag was observed (closed circles in Fig. 1B). Under condition (b), where Rho was preincubated with poly(C) RNA and then mixed with [α-^{32}P]ATP (squares in Fig. 1B), burst kinetics was observed. Under condition (c), where Rho protein was preincubated with [α-^{32}P]ATP for 10 s, and then rapidly mixed with poly(C) RNA to start the reaction, presteady state lag kinetics was observed, during which time no ATP hydrolysis was observed up to 0.3 s (open circles in Fig. 1B). After 0.3 s, ATP was hydrolyzed with linear kinetics at the poly(C) RNA-stimulated rate. The steady state rates under all three conditions were the same.

The absence of a burst, under condition where the reaction was initiated by mixing Rho with ATP plus RNA indicates that ATP and/or RNA-binding or ATP hydrolysis is rate limiting. The observation of a presteady state burst when Rho-RNA complex was preformed indicates that RNA binding is a slow step. When RNA is preincubated with Rho, a step associated with the ATP hydrolysis products (ADP + Pi) release becomes rate-limiting. The observation of a lag under condition where a Rho-ATP complex was preformed and the reaction was initiated by adding RNA is also consistent with RNA binding being rate-limiting. The lag time was unaffected by the concentration of ATP (data not shown), hence the lag was not due to slow ATP binding after the first turnover. We have previously reported detailed kinetics of RNA binding, and the stopped-flow studies have shown that RNA binds at a diffusion-limited rate but a competent Rho-RNA species is formed at a slow rate.[13] The lag kinetics therefore represents a slow initialization process, during which time RNA is loaded into the central channel of the Rho ring.[13] The presteady state ATP hydrolysis thus reflects the time required for the Rho hexamer to form the Rho-RNA complex that is competent in catalyzing multiple turnovers of steady state ATP hydrolysis. Therefore, a presteady state burst of ATP hydrolysis was observed only when the Rho protein was preincubated with the poly(C) RNA and reaction was initiated by the addition of ATP.

Burst Kinetics of ATP Hydrolysis by Three Nucleotide-Binding Sites of the Rho Hexamer. The results from the mixing experiments indicated that the Rho protein should be preincubated with the RNA in order to bypass the slow initiation steps related to RNA binding. We therefore investigated the presteady state ATPase kinetics in detail under condition (b). In the rapid quenched-flow kinetic experiment, 3.7 μM Rho (hexamer) and 5.0 μM poly(C) RNA were mixed with 500 μM ATP, and ADP formation was monitored after various times of mixing. The burst kinetics shown in Figure 2 were fit to a single exponential followed by a linear phase (Eq. 1) with a burst amplitude of 2.80 ± 0.28 ATP per hexamer, a burst rate constant of 30.7 ± 6.1 s^{-1}, and an ATPase turnover rate of 26.1 ± 0.96 ATP hydrolyzed s^{-1} $hexamer^{-1}$. Since Rho has six potential nucleotide-binding sites per hexamer, a hydrolysis burst of three ATPs per hexamer could result from irreversible hydrolysis of ATP at three active sites. Alternatively, the observed burst is lower than six because the ATPase reaction may be reversible at the six sites on Rho.[14] The absence of ^{18}O-exchange, which was reported previously,[6,15] indicates that ATP hydrolysis is irreversible on the enzyme active site. The acid-quench results therefore indicate that the Rho hexamer hydrolyzes three ATPs simultaneously at 500 μM ATP.

The rapid quenched-flow experiments were also performed at low [ATP]. No burst was observed at low [ATP], indicating that ATP binding is rate-limiting at low [ATP]. To

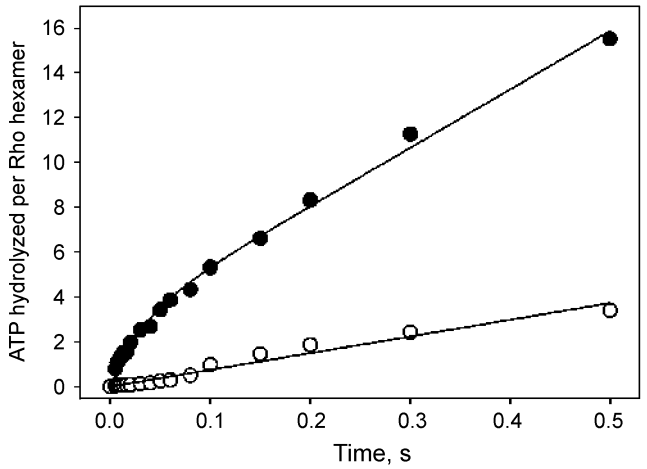

Figure 2. Presteady state acid-quenched kinetics of ATP hydrolysis at high and low [ATP]. A solution containing Rho hexamer (7.38 μM) and poly (C) RNA (10 μM) in the ATPase buffer was mixed with [α-^{32}P]ATP (40 μM and 1000 μM) in a rapid quenched-flow instrument at 18 °C, and the reaction was quenched with 2.0 M formic acid. The amount of ATP hydrolyzed to ADP per Rho hexamer was plotted as a function of time for both high [ATP] (500 μM final concentration, shown by closed circles) and low [ATP] (20 μM, shown by open circles). Continuous line onto the kinetics of ATP hydrolysis at 500 μM ATP represents fit of the burst equation (Eq. 1). Fitting parameters are shown in the text. Whereas, ATP hydrolysis kinetics obtained at 20 mM ATP was fit to the linear equation due to the absence of the burst.

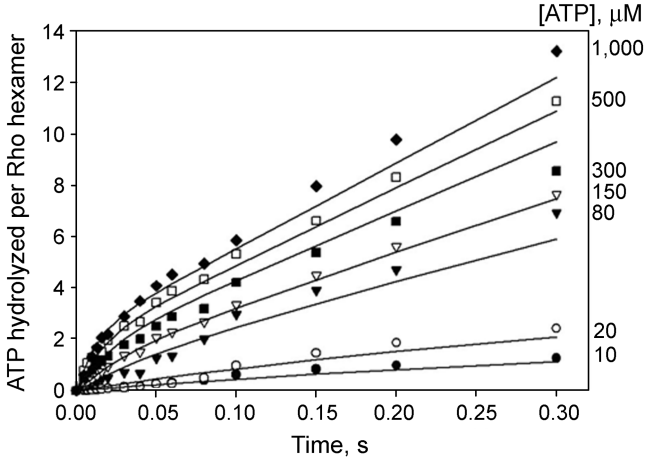

Figure 3. Presteady state kinetics of ATP hydrolysis by the Rho hexamer. Acid quenched-flow studies were performed in the ATPase buffer at 18 °C by mixing 7.38 μM Rho hexamer and 10 μM poly (C) RNA with excess ATP (20 μM-2.0 mM), followed by quenching with 2.0 M formic acid at the indicated times. These data were globally analyzed using the numerical analysis software to obtain the kinetic rate constants for step 1-3 for mechanism shown in Figure 5 and Table 1. The continuous lines overlaying the data are the simulated kinetic time courses for ATP hydrolysis by the Rho hexamer with three active sites based on Scheme 1 and the rate constants obtained from the global analysis, where k_1 = 4.4 × 10^5 $M^{-1}s^{-1}$, k_{-1} = 127 s^{-1}, k_2 = 88 s^{-1}, and k_3 = 12.9 s^{-1}.

investigate the ATP hydrolysis mechanism in more detail, the rapid acid quenched-flow experiments were repeated at various concentrations of ATP (Fig. 3). Each ATP hydrolysis time-course obtained at various [ATP] was fit to the burst equation (Eq. 1), and the fitting parameters were plotted against [ATP] as shown in Figure 4. The presteady state burst began to appear at [ATP] greater than 100 μM and increased with ATP concentration in a hyperbolic manner reaching a plateau of 3.8 ± 0.3 sites per hexamer with a $K_{1/2}$ of 197 ± 49 μM (Fig. 4A). The presteady state ATP hydrolysis rates were obtained either by taking initial slopes of the ATP hydrolysis kinetics during the first 30 msec (below 100 μM ATP) or by multiplying the burst amplitude and the burst rate (above 100 μM ATP). These rates were increased with [ATP] in a hyperbolic manner and reached a maximum rate constant of 181 ± 21 s^{-1} per Rho hexamer (Fig. 4B). The steady state ATPase rate increased with [ATP] and fit to a hyperbolic equation with a maximum ATPase rate constant of 34.5 ± 2.0 s^{-1} per hexamer and a $K_{1/2}$ of 32.3 ± 8.2 μM (Fig. 4C). This $K_{1/2}$ is close to the measured K_M of ATPase under similar experimental conditions; the reported steady state ATPase parameters are K_M = 29 μM and k_{cat} = 30.2 ± 2.5 s^{-1} per hexamer.[8,9]

Presteady State Kinetics of ATP Binding and Hydrolysis; A Three-Step Minimal Mechanism *via* Rapid Equilibrium ATP Binding. The presteady state kinetics at various [ATP] were fit to a minimal model shown in Scheme 1. It was assumed in this minimal mechanism that Pi release is a fast step because ^{18}O-exchange experiments showed that the ATPase reaction was not reversible.[15] The first step is the binding of ATP to the Rho-RNA complex with a bimolecular rate constant k_1, the HA complex dissociates into free H and A with a rate constant k_{-1}. ATP is hydrolyzed on the HA complex with a rate constant k_2 without reversibility (k_{-2} = 0), and k_3 is the rate constant of ADP release.

The kinetic data shown in Figure 3 were globally fit to the three-step ATP binding and hydrolysis mechanism using the computer program for numerical integration. The three-step model was expressed by the set of differential equations. The total product concentration at any time was expressed as the sum of enzyme-bound (HD) and free product (D) in the reaction: $[ADP]_{Tot}$ = HD + D. Numerical integration of the differential equations was used to fit the acid-quench ATPase kinetic data. Initial parameters were specified according to the reaction condition; [H] = 11.07 μM (3.69 μM Rho hexamer × 3 active sites), [HA] = [HD] = [D] = 0, and various [ATP] at time = 0. Estimates of the intrinsic rate constants were obtained from the analysis of the concentration dependence of the observed rate constants. The linear increase of the rates of presteady state ATP hydrolysis (dashed line in Fig. 4B) at low [ATP] provided an estimate of 2.9 × 10^5 $M^{-1}s^{-1}$, as the second-order rate constant for ATP binding (k_1). Estimate for the rate of hydrolysis step (k_2) was provided by the maximum rate of the ATP hydrolysis occurring in the presteady state phase, 180 s^{-1} (Fig. 4B). Initial value for the product release step was estimated to be 11 s^{-1} by dividing V_{max} of steady state ATP hydrolysis with the concentration of enzyme active sites (Fig. 4C), because the product release step is likely to limit the steady state catalytic process at high [ATP] as substantiated by the

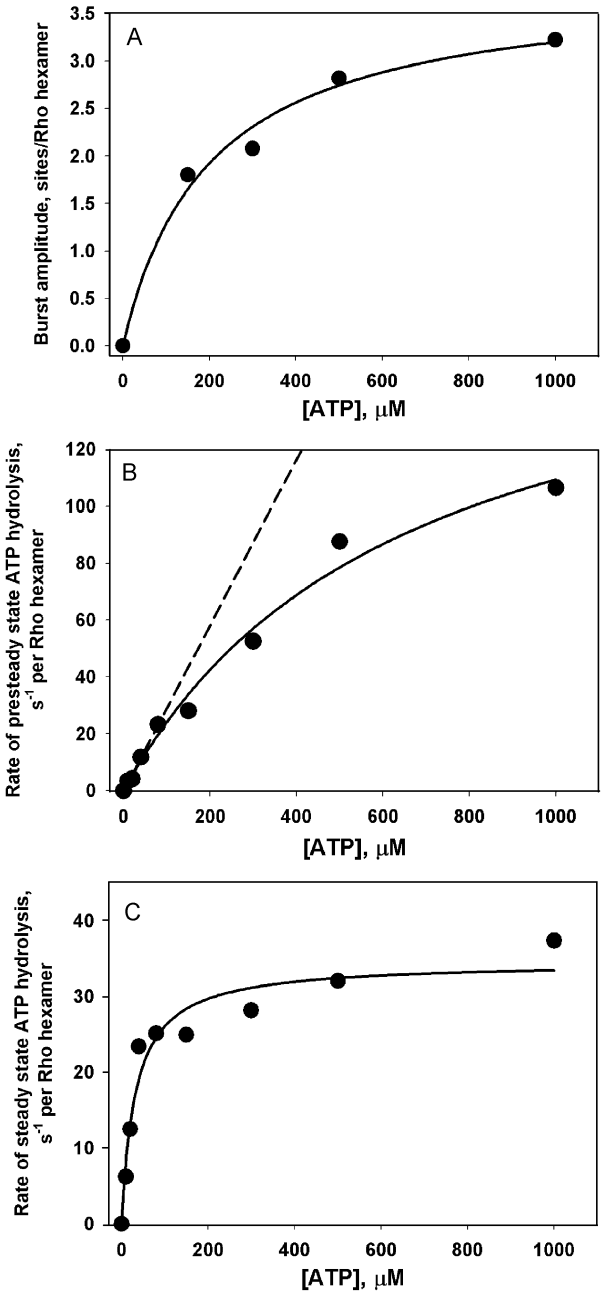

Figure 4. The [ATP] dependence of the presteady state kinetics of ATP hydrolysis. (A) shows the [ATP] dependence of the burst amplitude. The presteady state ATP hydrolysis burst was observed at [ATP] higher than 100 μM. The presteady state burst amplitude was obtained by applying the burst equation (Eq. 1). The burst amplitude increased with [ATP] in a hyperbolic manner and achieved a plateau value of 3.8 ± 0.3 sites per Rho hexamer with a $K_{1/2}$ of 197 ± 49 μM. (B) shows the [ATP] dependence of the presteady state ATP hydrolysis rate. The burst rate constants were obtained from the initial slope of ATP hydrolysis kinetics prior to the reaction reaching the steady state. Presteady state burst rates increased with [ATP] in a hyperbolic manner and reached a maximum rate constant of 181 ± 21 s^{-1} per hexamer with a $K_{1/2}$ of 649 ± 143 μM. Dashed line represents a linear increase of the rates at low [ATP] with a slope of 2.9×10^5 $M^{-1}s^{-1}$. (C) shows the [ATP] dependence of the steady state ATP hydrolysis rate. The [ATP] dependence of the ATPase turnover rate fit to a hyperbolic equation with a maximum ATPase rate constant of 34.5 ± 2.0 s^{-1} per hexamer and a $K_{1/2}$ of 32.3 ± 8.2 μM.

Table 1. Intrinsic rate constants characterizing presteady state ATP binding and hydrolysis by the *E. coli* Rho. Rate constants were determined using the following kinetic model (Scheme 1) for global fitting of acid quenched-flow ATPase kinetic data sets at various [ATP]. In the following scheme H represents the Rho-RNA complex with three active sites; A represents ATP, and D represents ADP

$$H + A \underset{k_{-1}}{\overset{k_1}{\rightleftharpoons}} HA \xrightarrow{k_2} HD \xrightarrow{k_3} H + D$$

	Initial estimates[a]	Global fit[b]
k_1 ($M^{-1}s^{-1}$)	2.9×10^5	4.4×10^5
k_{-1} (s^{-1})	Not available	127
k_2 (s^{-1})	180	87.7
k_3 (s^{-1})	11	12.9
K_d (μM)[c]		290
K_1k_2 ($M^{-1}s^{-1}$)[d]		3.0×10^5

[a]These rate constants, obtained by analysis of the [ATP] dependencies of the observed rate constants (Fig. 4), were used as estimates for the intrinsic rate constants during global fitting (Fig. 3). [b]Final values for the intrinsic rate constants were obtained by global fitting data sets at increasing [ATP]. [c]Equilibrium dissociation constant was obtained by k_{-1}/k_1. [d]K_1k_2 gives the apparent second-order rate constant for ATP binding ($K_1 = 1/K_d$).

appearance of burst kinetics of ATP hydrolysis.

The continuous lines in Figure 3 are numerical fits of the kinetic data at various ATP concentrations to the three-step mechanism. Four intrinsic rate constants were derived from the global fitting and summarized in Table 1. The intrinsic rate constants indicate that the rate of dissociation from the collision complex (HA), defined by k_{-1}, is much faster than k_2, the rate constant of chemical reaction. Under this condition the binding in the first step comes to equilibrium on a time scale much faster than the first-order chemistry step. Thus, the first step can be simplified as a rapid-equilibrium reaction mechanism (Scheme 2):

$$H + A \overset{K_1}{\rightleftharpoons} HA \xrightarrow{k_2} HD \xrightarrow{k_3} H + D \quad \text{(Scheme 2)}$$

The apparent dissociation constant, $K_d = 1/K_1$, was calculated to be 290 μM by dividing the *off* rate (k_{-1}) with the *on* rate (k_1). According to this mechanism the apparent second-order rate constant for ATP binding is given by the product K_1k_2, which is equal to 3.0×10^5 $M^{-1}s^{-1}$. Note that the calculated rate constant for ATP binding is close to the estimated apparent *on* rate ($k_{on} = 2.9 \times 10^5$ $M^{-1}s^{-1}$) by taking the initial slope of the presteady state rate of ATP hydrolysis as a function of [ATP] (Fig. 4B). These results suggest that during the initial presteady state time period three ATPs bind to Rho hexamer *via* rapid equilibrium prior to hydrolysis and are subsequently hydrolyzed and released, which is followed by steady state ATPase turnovers.

Discussion

The studies reported here revealed the kinetic mechanism of ATP binding and hydrolysis by the Rho hexamer complexed with RNA during the initiation process. Previous

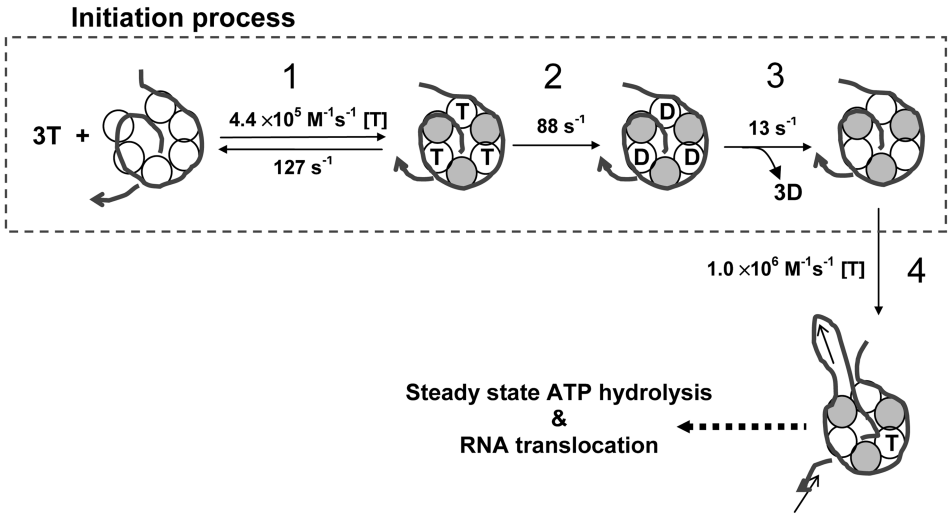

Figure 5. A proposed kinetic model summarizing the presteady state kinetics of ATP binding and hydrolysis by Rho-RNA complex. The model shows the possible kinetic intermediates and rate constants in the pathway of ATP binding and hydrolysis by the Rho hexamer during the initialization step prior to the steady state ATPase turnovers. RNA strand was drawn as a continuous line with an arrow to designate 3'-end. ATP and ADP were shown as T and D, respectively. See the text for detail.

studies showed that the RNA needs to travel into the central channel of the Rho hexamer to stimulate the ATPase activity.[13] To this end, RNA strand initially needs to be properly located in the Rho hexamer to prime the steady state ATPase reaction. Therefore, the results of the presteady state ATP hydrolysis kinetics shown in this study suggest that the initial burst of ATP hydrolysis in the Rho-RNA complex is required for the formation of a competent Rho-RNA complex that can catalyze multiple ATPase turnovers.

Conformational Transitions of the Rho-RNA Complex Occur prior to the Steady State ATPase Turnovers. The presteady state ATP hydrolysis studies using the acid quenched-flow methods indicate that binding of the ATP to the three to four sites is required for the initialization process of the Rho-RNA complex. The apparent second-order rate constant for ATP binding (2.9×10^5 $M^{-1}s^{-1}$) obtained from presteady state ATPase kinetics, which limits the presteady state ATP hydrolysis phase, is slower than the k_{cat}/K_m (1.0×10^6 $M^{-1}s^{-1}$), which sets the lower limit for substrate binding for steady state ATPase turnovers at 18 °C. This result suggests the ATP binding/hydrolysis pathway during the presteady state time period is different with the one that occurs during the steady state time period. Therefore, we propose that the first three ATP binding and simultaneous hydrolysis are engaged in the initialization process, in which Rho-RNA complex may undergo conformational change(s) in the presence of ATP, prior to the subsequent steady state ATPase turnovers. Here we assumed that these conformational changes of Rho-RNA complex, induced by nucleotide binding and hydrolysis occurring in the presteady state time period, are initialization events. This type of conformational changes induced by nucleotide binding has been observed in DnaB helicase. Binding of nucleotide cofactors to the DnaB induces global conformational changes of the hexamer,[16,17] and occurs through the sequential mechanism with accompanying protein conformational changes.[18]

Kinetic Pathway for ATP Binding and Hydrolysis by the Rho-RNA Complex during Initiation Process. A kinetic model for how Rho-RNA complex undergoes several conformational changes utilizing ATP binding/hydrolysis was proposed based on the results obtained in this study as well as the previous reports.[9,13,19] The model (Fig. 5) shows the possible intermediate structures of Rho-RNA complex in the pathway of ATP binding and hydrolysis by the Rho hexamer. The shaded subunits depict noncatalytic sites that are not involved in the presteady state and steady state ATP hydrolysis.[9] Rho hexamer adapts its "lock-washer" conformation prior to RNA loading onto the hexameric ring, and the Rho hexamer closes its ring by accommodating the RNA into the central channel of the protein.[3-5] During this initialization process ATP binding has been implicated for attaining a proper protein conformation.[19] Rho hexamer was thus assumed to be inactive with C_6 configuration until the first ATP hydrolysis occurs. This model involves the following steps; 1) three ATPs bind to the Rho-RNA complex *via* a rapid-equilibrium with a bimolecular rate of 4.4×10^5 M^{-1} s^{-1} and a dissociation rate of 127 s^{-1}; 2) three ATP molecules get hydrolyzed at a rate close to 88 s^{-1}; 3) three ADPs dissociate from the active sites at a slow rate of 13 s^{-1}, and the presteady state initialization process is completed; 4) ATP binds to the catalytic site at a rate of 1.0×10^6 $M^{-1}s^{-1}$ that was derived from the steady state ATPase parameters (k_{cat}/K_m), by which Rho protein undertakes the catalytic cycle of steady state ATP hydrolysis and translocate along the RNA strand. Rate constants of step 1-step 3 are obtained by the global fitting of the presteady state ATP hydrolysis kinetic data (Fig. 3 & 4 and Table 1).

In this study the presteady state ATPase kinetics was carried out by adding RNA to start the reaction. Under these conditions (Setup c in Fig. 1), we observed a long lag that

suggests that RNA binding is a slow step. Therefore, under these conditions, one measures the ATPase kinetics associated with the initiation process rather than the ATPase kinetics during steady state. Thus, investigation of the presteady state ATP hydrolysis kinetics of the Rho protein monitors the initiation process of the Rho-RNA complex for subsequent steady state ATPase cycle. It would be also interesting to compare ATPase kinetics by monitoring protein fluorescence change accompanied by ATP binding and subsequent hydrolysis.[20] Our study indicates that the first turnover of ATP hydrolysis by the Rho hexamer is unique and largely dictated by the initiation process that may involve protein conformational changes and proper binding of the RNA to the Rho hexamer.

Acknowledgment. This work was supported by the Korea Research Foundation Grant funded by the Korean Government (MOEHRD) R05-2004-000-11524-0.

References

1. Brennan, C. A.; Dombroski, A. J.; Platt, T. *Cell* **1987**, *48*, 945.
2. Geiselmann, J.; Wang, Y.; Seifried, S. E.; von Hippel, P. H. *Proc. Natl. Acad. Sci. USA* **1993**, *90*, 7754.
3. Bogden, C. E.; Fass, D.; Bergman, N.; Nichols, M. D.; Berger, J. M. *Molecular Cell* **1999**, *3*, 487.
4. Burgess, B. R.; Richardson, J. P. *J. Biol. Chem.* **2001**, *276*, 41.
5. Richardson, J. P. *Cell* **2003**, *114*, 157.
6. Stitt, B. L. *J. Biol. Chem.* **1988**, *263*, 11130.
7. Geiselmann, J.; von Hippel, P. H. *Protein Sci.* **1992**, *1*, 850.
8. Kim, D. E.; Patel, S. S. *J. Biol. Chem.* **1999**, *274*, 32667.
9. Kim, D. E.; Shigesada, K.; Patel, S. S. *J. Biol. Chem.* **1999**, *274*, 11623.
10. Mori, H.; Imai, M.; Shigesada, K. *J. Mol. Biol.* **1989**, *210*, 39.
11. Finger, L. R.; Richardson, J. P. *Biochemistry* **1981**, *20*, 1640.
12. Geiselmann, J.; Yager, T. D.; von Hippel, P. H. *Protein Sci.* **1992**, *1*, 861.
13. Kim, D. E.; Patel, S. S. *J. Biol. Chem.* **2001**, *276*, 13902.
14. Johnson, K. A. *Methods in Enzymology* **1995**, *249*, 38.
15. Stitt, B. L.; Xu, Y. *J. Biol. Chem.* **1998**, *273*, 26477.
16. Yu, X.; Jezewska, M. J.; Bujalowski, W.; Egelman, E. H. *J. Mol. Biol.* **1996**, *259*, 7.
17. Jezewska, M. J.; Bujalowski, W. *J. Biol. Chem.* **1996**, *271*, 4261.
18. Bujalowski, W.; Jezewska, M. J. *Biochemistry* **2000**, *39*, 2106.
19. Jeong, Y. J.; Kim, D. E.; Patel, S. S. *J. Biol. Chem.* **2004**, *279*, 18370.
20. Kim, J.; Choi, J.-D.; Kim, B.-H.; Yoon, M.-Y. *Bull. Kor. Chem. Soc.* **2005**, *26*, 260.